JACS
JOURNAL OF THE AMERICAN CHEMICAL SOCIETY

Communication

pubs.acs.org/JACS

Magnetic Field-Activated Sensing of mRNA in Living Cells

Saira F. Bakshi,[†] Nataliia Guz,[†] Andrey Zakharchenko,[§] Han Deng,[‡] Alexei V. Tumanov,[∥] Craig D. Woodworth,[‡] Sergiy Minko,[*,§] Dmitry M. Kolpashchikov,[*,#,⊥] and Evgeny Katz[*,†]

[†]Department of Chemistry and Biomolecular Science, Clarkson University, Potsdam, New York 13699-5810, United States

[§]Nanostructured Materials Lab, University of Georgia, Athens, Georgia 30602, United States

[‡]Department of Biology, Clarkson University, Potsdam, New York 13699-5810, United States

[∥]Department of Microbiology, Immunology, and Molecular Genetics, University of Texas Health Science Center at San Antonio, 7703 Floyd Curl Drive, San Antonio, Texas 78229-3900, United States

[#]Chemistry Department, University of Central Florida, 4000 Central Florida Boulevard, Orlando, Florida 32816-2366, United States

[⊥]Laboratory of Solution Chemistry of Advanced Materials and Technologies, ITMO University, Lomonosova St. 9, 191002 St. Petersburg, Russian Federation

Supporting Information

ABSTRACT: Detection of specific mRNA in living cells has attracted significant attention in the past decade. Probes that can be easily delivered into cells and activated at the desired time can contribute to understanding translation, trafficking and degradation of mRNA. Here we report a new strategy termed magnetic field-activated binary deoxyribozyme (MaBiDZ) sensor that enables both efficient delivery and temporal control of mRNA sensing by magnetic field. MaBiDZ uses two species of magnetic beads conjugated with different components of a multicomponent deoxyribozyme (DZ) sensor. The DZ sensor is activated only in the presence of a specific target mRNA and when a magnetic field is applied. Here we demonstrate that MaBiDZ sensor can be internalized in live MCF-7 breast cancer cells and activated by a magnetic field to fluorescently report the presence of specific mRNA, which are cancer biomarkers.

The development of green fluorescent protein (GFP) for intracellular imaging of specific proteins was acknowledged by a Nobel Prize in Chemistry in 2008.[1] Imaging of specific mRNA inside individual cells is another important task that can contribute to both understanding of mRNA processing and to probing the functions of recently discovered noncoding RNAs.[2] A great variety of approaches for targeted sensing of mRNA in live cells has been proposed in recent years including aptamer-protein systems (e.g., MS2 system),[3] aptamer-dye systems (e.g., spinach aptamer),[4] nucleic acid templated chemical reactions,[5] adjacent hybridization probes,[6] molecular beacon (MB) probes[7] and nanoparticle-based approaches,[8,9] among others.[10] However, the delivery of the probes or expression of fluorescent species within genetically modified cells requires hours of incubation. Development of a probe that could be activated with a remotely applied physical stimulus would enable activation of sensing and quantification of mRNA in cells at the desired time point. Caged MB probes have been suggested for light-activated detection, which can potentially enable temporal control of sensing.[11] However, caged MB probes produce high background fluorescence[11b,12] and require invasive delivery of the probe inside cells.[13] Moreover, light-dependent activation may result in either incomplete probe activation or photodamage to living cells. Therefore, no efficient approaches for instant, remotely activated sensing of mRNA inside cells are available to date.

Nanomagnetic actuation[14] (activation of biomolecular species bound to magnetic nanoparticles in the presence of an externally applied magnetic field) elegantly addresses the common issues faced by other comparative techniques for the remote sensing and actuation of intracellular processes. Indeed, owing to its high precision and accuracy, the coupling of a magnetic field to a biomolecule-conjugated magnetic nanoparticle has been applied to several areas of biomedical science: for the investigation of cell mechanical properties,[15] mechanosensitive ion channel signaling pathways,[16] and for targeted activation of specific ion channels.[17]

Here we report a new RNA sensing technology based on the principles of nanomagnetic actuation, magnetic field-activated binary deoxyribozyme (MaBiDZ), which enables sensing of a specific mRNA analyte via application of a magnetic field in a remote and noninvasive manner. The technology takes advantage of magnetic beads (MaB) coupled to a binary deoxyribozyme (BiDZ) probe (Scheme 1A), developed earlier.[18] BiDZ consists of three components: the analyte binding arms (DZa and DZb) and a fluorogenic reporter substrate (F-sub). F-sub is an oligonucleotide strand composed of a fluorophore and quencher conjugated to the opposite sides of the cleavage site. DZa and DZb can hybridize to a specific DNA or RNA analyte and form the DZ catalytic core, which cleaves F-sub, thus resulting in separation of the fluorophore and quencher followed by fluorescent signaling. Important advantages of BiDZ over other hybridization probes is its improved sensitivity, single mismatch selectivity at ambient temperatures, simple design, and low cost.[18] In this work, we took advantage of the modular design and high sensitivity of the BiDZ probe

Received: June 10, 2017
Published: August 17, 2017

DOI: 10.1021/jacs.7b06022
J. Am. Chem. Soc. 2017, 139, 12117−12120

Scheme 1. Principle of Magnetic Field-Activated Deoxyribozyme Sensor[a]

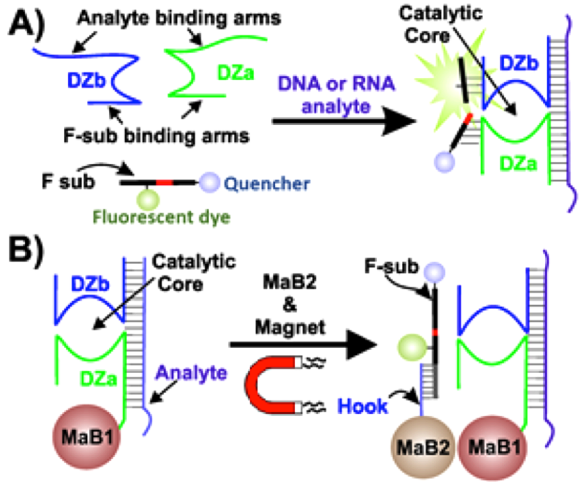

[a](A) Binary deoxyribozyme sensor (BiDZ) as reported earlier.[18] DNA strands DZa and DZb hybridize to adjacent position of analyte and form deoxyribozyme catalytic core, which cleaves fluorogenic F-sub and increases sample fluorescence. (B) MaBiDZ developed in this study. Magnetic bead (MaB1)-bound DZa forms a catalytic core with DZb in the presence of analyte. The activated sensor produces signal only when: (i) second species of magnetic beads, MaB2 carrying F-sub is present and (ii) magnetic field that aggregates MaB1 and MaB2 is applied. See the DNA sequences in Table 1.

for the development of MaBiDZ, a novel magnetic field-activated switch for real time mRNA sensing in live cells.

The magnetic switch consists of two species of 100 nm magnetic beads (MaB), MaB1 and MaB2 (Scheme 1B). MaB is composed of a 15 nm iron oxide (Fe_3O_4) superparamagnetic core encased in a silica shell. The shell is modified with a grafted polymeric brush of a block copolymer PAA-*b*-PEGMA composed of poly(acrylic acid) (PAA) and a polymer of poly(ethylene glycol) methyl ether acrylate (PEGMA). The MaB cores have a saturation magnetization value (47 emu/g),[19] which is sufficient for effective utilization of magnetic force. The DNA strands are conjugated to MaB via the polymeric brush using a flexible linker, which is known to improve biocompatibility, facilitate intracellular delivery and prevent nanoparticle aggregation in the absence of a magnetic field,[20] whereas the flexible linker allows mobility of the BiDZ arms.

MaBiDZ consists of the DZb strand, MaB1 conjugated with DZa and MaB2 conjugated with DNA hook strand complementary to F-sub (Scheme 1B, see SI for details of the conjugation procedure). F-sub is incubated with the Hook-MaB2 conjugate, which is then rinsed to remove unbound F-sub. A DNA or RNA analyte hybridized to DZa and DZb strands enables formation of the DZ catalytic core. The catalytic core does not produce the fluorescent signal unless hybridized with F-sub. Application of an external magnetic field induces aggregation of the MaB1 and MaB2, thus bringing the activated BiDZ sensor in close proximity to F-sub, which is followed by F-sub cleavage and amplification of fluorescent signal. Though the 3D motion of MaBiDZ may be restricted under a magnetic field, both the flexible linker and large particle size allow a greater degree of contact points between the two DZ species. To the best of our knowledge this is the first strategy that allows activation of a hybridization sensor by a magnetic field. Another important advantage of this approach is the low background fluorescence due to the low concentration of the F-sub in solution, in comparison with the BiDZ detection (Scheme 1A). Indeed, the amount of F-sub attached to the beads is much lower than that used by BiDZ sensor (typically 200 nM). However, when MaB1 and MaB2 are aggregated, the local concentration of F-sub near the activated sensor is high.

For the proof-of-concept study, we chose to target Twist mRNA. Twist is a helix−loop−helix transcription factor whose overexpression has been shown to contribute to metastasis by promoting an epithelial-mesenchymal transition.[21] Thus, an intracellular sensor that can fluorescently report Twist mRNA levels would be useful to assess metastatic potential of cells in clinical applications. We first optimized the performance of the sensor in *in vitro* experiments using a synthetic DNA analyte with the sequence of Twist mRNA (see Twist sequence in Table 1).

Table 1. Oligonucleotides Used in the Study

Name[a]	Sequences
F-sub	5′-CGGT ACA TTG TAG AAG TT AAG GTT^{FAM} TCC TCg uCC CTG GGC A-BHQ1
Twist	5′-TAGT GGG ACG CGG ACA TGG ACC AGG CCC CCT CCA TCC TCC AGA CCG AGA AGG CGT AGC TGA GCC GCT CGT GAG CCA CAT AGC TGC A
DZa	5′-NH_2/AAA AAA AAA AAA AAA AAA AAC GAG CGG CTC AGC TAC GCC T AC AAC CGA GAG AGG AAA C
DZb	5′-CCA GGG A GG CTA GCT TCT CGG TCT GGA GGA TGG AG
Hook	5′-NH_2/AAA AAA AAA AAA AAA AAA AA/iSp9/AAC TTC TAC AAT GTA CCG

[a]iSp9 - triethylene glycol linker; FAM attached to the DNA is a fluorescein derivative; BHQ1 - "Black Hole Quencher" is a fluorescence quencher; ribonucleotides are in low case.

The results of *in vitro* studies demonstrated a near 2-fold enhancement of fluorescent signal when MaBiDZ is switched ON in the presence of the magnetic field compared to the OFF state, for which the signal does not change over time (Figure 1A). Importantly, the signal remained at the background level in the absence of an applied magnetic field (Figure 1A, (c)) and in the absence of analyte (Figure 1A, (b)). Furthermore, the

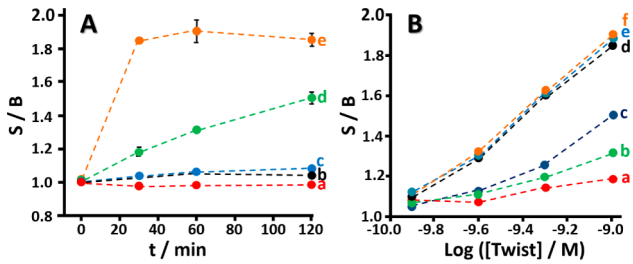

Figure 1. Comparison of *in vitro* fluorescent response of BiDZ and MaBiDZ sensor systems. (A) Time dependent response of BiDZ and MaBiDZ sensor: (a) without F-sub, (b) without synthetic Twist (see Table1) analyte, (c) response of MaBiDz without magnet applied, (d) response of BiDZ, and (e) MaBiDZ activated with magnetic field in the presence of 1 nM synthetic Twist analyte (see SI for concentrations of all other components of the BiDZ and MaBiDZ probe.) (B) Response of MaBiDZ (d, e, f) compared to BiDZ (a, b, c) in the presence of different concentrations of Twist analyte after 30 (a,d), 60 (b,e) or 120 (c,f) min. All error bars are the result of three independent measurements; some bars are not visible because they are smaller than the labels for the experimental points.

DOI: 10.1021/jacs.7b06022
J. Am. Chem. Soc. 2017, 139, 12117−12120

signal response to a noncomplementary target is similar to that of the background fluorescence (see SI for Figure SI5). The results also demonstrate faster activation of MaBiDZ compared to BiDZ, (Figure 1A, compare slopes of lines e and d). Time dependent profiles demonstrate that unlike BiDZ, MaBiDZ does not demonstrate time dependence of fluorescent response, but produces maximum signal within 30 min. These data demonstrate important advantages of MaBiDZ system in comparison with BiDZ: (1) it responds faster upon activation by magnetic field and reaches maximum signal in shorter time, due to, presumably, higher local concentration of F-sub. MaBiDZ's response does not increase over longer incubation time due to the shortage of F-sub supply, which is limited by contact area between MaB1 and MaB2. Thus, an important feature of the MaBiDZ system is activation at the desired time. (2) The two-probe system allows measurement of Twist in a controlled fashion by separating F-sub and DZa, lowering the background signal generated.

Next we chose to test the sensing ability of MaBiDZ *ex vivo* in mammalian cell culture. We chose the MCF-7 breast cancer cell line, and human cervical epithelial cells (HCX) isolated from human tissue, which express high[22] and lower levels[23] of Twist mRNA, respectively. Our first aim was to compare the fluorescent response of MaBiDZ in MCF-7 cells with and without exposure to a magnetic field (ON and OFF states, respectively) using confocal laser scanning microscopy (CLSM). Cells were incubated with MaBiDZ at a 40 μg/mL concentration (within the none-toxicity concentration range, see Figure SI9) for 4 h and monitored with CLSM every 30 min. Cells exposed to a magnetic field demonstrated a highly fluorescent response compared to those without a magnetic field (compare green fluorescence in panels A and C, Figure 2). Next, we tested MaBiDZ in its ability to detect different levels of mRNA. CLSM images demonstrated higher fluorescent responses in MCF-7 (panel A and C) than in HCX (panel B and D) cells consistent with the reported differences in Twist mRNA levels.[22,23]

To quantify the intracellular signaling of the MaBiDZ probe, we examined large population of cells treated with probes using flow cytometry. This method eliminates variations that can be observed using CLSM, which only permits the examination of a small fraction of cells. Flow cytometry results (Figure 2, insets) show that MCF-7 cells treated with MaBiDZ and a magnetic field (ON state) exhibited 4 times greater fluorescence than MaBiDZ-treated MCF-7 cells without a magnetic field (OFF state), thus confirming the magnetic field-dependent switch-like effect of this system (compare insets in Figure 2A,C). When compared to the control noncancerous HCX cells, MCF-7 cells exhibited a 20-fold fluorescence enhancement (compare panel A with B, in Figure 2). It is important to note that significant signaling was apparent after only 2.5 h, as opposed to a previous technique that required an incubation of 12 h before a signal could be detected.[9] To demonstrate the low background of MaBiDZ, we incubated MaB2 (bound to F-sub) alone in MCF-7 cells (see SI, Figure SI6). A signal enhancement was not observed, confirming that MaB-attachment protects F-sub from nuclease-induced cleavage, which would result in high background fluorescence. Earlier, a similar effect was observed for gold nanoparticle-attached fluorescent probes.[8] The fluorescence data from CLSM and flow cytometry measurements of whole cells was validated using fluorescence data of cell lysates (see SI, Figure SI10). This data was in good agreement with measurements of Twist levels from whole cells.

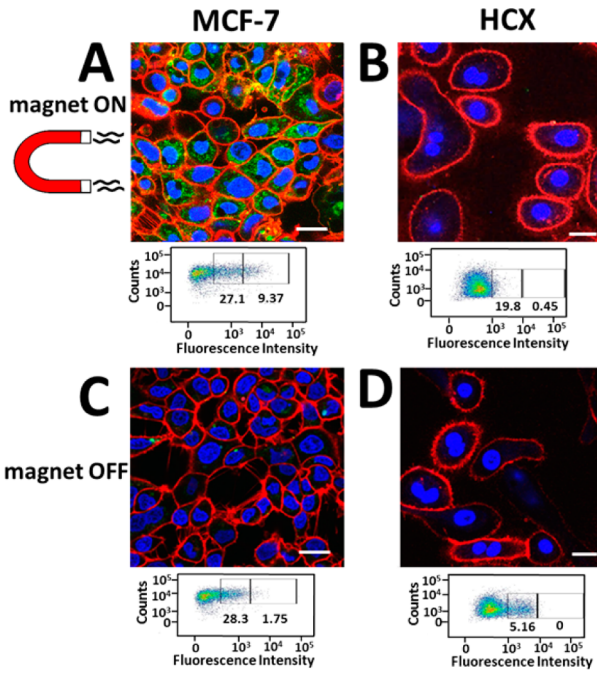

Figure 2. Intracellular testing of MaBiDZ sensor. CLSM images of (A) Twist-overexpressing MCF-7 cancer cells treated with MaBiDZ sensor with magnetic field applied and (C) no magnetic field applied. Analogously treated cervical epithelial cells (expressing low levels of Twist) with (B) magnetic field applied and (D) without magnetic field. Images were taken after 2.5 h of incubation time. Nuclei are stained with Hoechst nuclear stain and visualized with 408 nm laser. Surfaces are stained with anti-epithelial cell adhesion molecule (EpCAM) antibody and visualized with a 635 nm laser. Fluorescence from the MaBiDZ probe is visualized with the 488 nm laser. Corresponding flow cytometry data are shown as insets below each image. The gates on flow cytometry plots indicate percent of EpCAM positive cells with low and high MaBiDZ fluorescence. The number of internalized particles was estimated to be ca. 1×10^6 MaBiDZ per cell (see Figure SI11). Scale bar is 20 μm.

Our next aim was to investigate the mechanisms that promote the observed signaling efficiency and enhancement of MaBiDz within the cell. We hypothesized that the magnetic field plays a role in enhancing cellular entry and intracellular transport kinetics, based on previous reports.[24] To investigate this, we examined a small window of events upon cellular entry of MaBiDZ, both with (ON) and without (OFF) a magnetic field. Previous studies[25] show that nanoparticles enter cells by endocytosis, and are subsequently either stored in endosomes or lysosomes, or undergo endosomal escape. If these intracellular nanoparticles cannot escape from the endosome or lysosome, they are not available for intracellular sensing. Therefore, we investigated the distribution and colocalization of the oligo-modified MaBs and endosomes by CLSM at various time points. Results indicate that, at the peak of endosomal internalization of MaB, the ON state demonstrated about 50% less colocalization of MaB and endosomes compared to the OFF state (see SI for Figures SI7–8). Though the mechanism is under investigation, the data suggest that a magnetic field mitigates the bottleneck of endosomal sequestering, freeing nanoparticles for sensing functions in the cytoplasm.

In summary, we have designed a fluorescent hybridization MaBiDZ mRNA sensing system that can be activated by a magnetic field at the desired time. MaBiDZ sensing technology produces low backround fluorescence that can be instantly

DOI: 10.1021/jacs.7b06022
J. Am. Chem. Soc. 2017, 139, 12117–12120

activated by magnetic field. We demonstrated that the sensor can be used for magnetic field-dependent mRNA sensing in living cells. The technology enables detection of specific mRNA in live cells within 2.5 h after applying a magnetic field, which is a significant improvement in comparison with current techniques. We hope that the MaBiDZ technology introduced here will add to the toolbox of techniques for RNA analysis in live cells. The developed approach can find much broader applications than the presently demonstrated cancer biomarker analysis example.

■ ASSOCIATED CONTENT

Supporting Information

The Supporting Information is available free of charge on the ACS Publications website at DOI: 10.1021/jacs.7b06022.

Details of experimental procedures, complete structure of probe-analyte complex, and control experiments with cell culture (PDF)

■ AUTHOR INFORMATION

Corresponding Authors

*ekatz@clarkson.edu
*dmitry.kolpashchikov@ucf.edu
*sminko@uga.edu

ORCID

Alexei V. Tumanov: 0000-0001-6042-0152
Sergiy Minko: 0000-0002-7747-9668
Dmitry M. Kolpashchikov: 0000-0002-8682-6553
Evgeny Katz: 0000-0002-1618-4620

Notes

The authors declare no competing financial interest.

■ ACKNOWLEDGMENTS

This work at Clarkson University (E.K.) and at the University of Georgia (S.M.) was supported by the NSF awards CBET-1403208 and DMR-1309469. The work at University of Central Florida (D.M.K.) and Clarkson (C.D.W.) was supported by NIH awards R15AI10388001A1 and 1R15CA173703-01. D.M.K. was partially supported by the ITMO University Fellowship and Professorship Program.

■ REFERENCES

(1) Germond, A.; Fujita, H.; Ichimura, T.; Watanabe, T. M. *Biophys. Rev.* **2016**, *8*, 121−138.

(2) (a) Cui, M.; You, L.; Ren, X.; Zhao, W.; Liao, Q.; Zhao, Y. *Biochem. Biophys. Res. Commun.* **2016**, *471*, 10−14. (b) Guo, D.; Barry, L.; Lin, S. S. H.; Huang, V.; Li, L.-C. *RNA Biol.* **2014**, *11*, 1221−1225. (c) Qi, X.; Zhang, D.-H.; Wu, N.; Xiao, J.-H.; Wang, X.; Ma, W. *J. Med. Genet.* **2015**, *52*, 710−718.

(3) Bertrand, E.; Chartrand, P.; Schaefer, M.; Shenoy, S. M.; Singer, R. H.; Long, R. M. *Mol. Cell* **1998**, *2*, 437−445.

(4) Paige, J. S.; Wu, K. Y.; Jaffrey, S. R. *Science* **2011**, *333*, 642−646.

(5) (a) Holtzer, L.; Oleinich, I.; Anzola, M.; Lindberg, E.; Sadhu, K. K.; Gonzalez-Gaitan, M.; Winssinger, N. *ACS Cent. Sci.* **2016**, *2*, 394−400. (b) Michaelis, J.; Roloff, A.; Seitz, O. *Org. Biomol. Chem.* **2014**, *12*, 2821−2833. (c) Franzini, R. M.; Kool, E. T. *Bioconjugate Chem.* **2011**, *22*, 1869−1877.

(6) Santangelo, P. J.; Nix, B.; Tsourkas, A.; Bao, G. *Nucleic Acids Res.* **2004**, *32*, e57.

(7) (a) Zhao, D.; Yang, Y.; Qu, N.; Chen, M.; Ma, Z.; Krueger, C. J.; Behlke, M. A.; Chen, A. K. *Biomaterials* **2016**, *100*, 172−183. (b) Giraldo-Vela, J. P.; Kang, W.; McNaughton, R. L.; Zhang, X.; Wile, B. M.; Tsourkas, A.; Bao, G.; Espinosa, H. D. *Small* **2015**, *11*, 2386−2391.

(8) Seferos, D. S.; Giljohann, D. A.; Hill, H. D.; Prigodich, A. E.; Mirkin, C. A. *J. Am. Chem. Soc.* **2007**, *129*, 15477−15479. (a) Prigodich, A. E.; Seferos, D. S.; Massich, M. D.; Giljohann, D. A.; Lane, B. C.; Mirkin, C. A. *ACS Nano* **2009**, *3*, 2147−2152. (b) Zheng, D.; Seferos, D. S.; Giljohann, D. A.; Patel, P. C.; Mirkin, C. A. *Nano Lett.* **2009**, *9*, 3258−3261. (c) Pan, W.; Li, Y.; Wang, M.; Yang, H.; Li, N.; Tang, B. *Chem. Commun.* **2016**, *52*, 4569−4572.

(9) Briley, W. E.; Bondy, M. H.; Randeria, P. S.; Dupper, T. J.; Mirkin, C. A. *Proc. Natl. Acad. Sci. U. S. A.* **2015**, *112*, 9591−9595.

(10) (a) Feyder, M.; Goff, L. A. *J. Clin. Invest.* **2016**, *126*, 2783−2791. (b) Ouellet, J. *Front. Chem.* **2016**, *4*, No. 29. (c) Shigeto, H.; Nakatsuka, K.; Ikeda, T.; Hirota, R.; Kuroda, A.; Funabashi, H. *Anal. Chem.* **2016**, *88*, 7894−7898. (d) Takahashi, K.; Ito, S.; Nakamoto, K.; Ito, Y.; Ueno, Y. *J. Org. Chem.* **2015**, *80*, 8561−8570. (e) Urbanek, M. O.; Galka-Marciniak, P.; Olejniczak, M.; Krzyzosiak, W. J. *RNA Biol.* **2014**, *11*, 1083−1095.

(11) (a) Wang, C.; Zhu, Z.; Song, Y.; Lin, H.; Yang, C. J.; Tan, W. *Chem. Commun.* **2011**, *47*, 5708−5710. (b) Joshi, K. B.; Vlachos, A.; Mikat, V.; Deller, T.; Heckel, A. *Chem. Commun.* **2012**, *48*, 2746−2748. (c) Rinne, J. S.; Kaminski, T. P.; Kubitscheck, U.; Heckel, A. *Chem. Commun.* **2013**, *49*, 5375−5377.

(12) (a) Ruble, B. K.; Yeldell, S. B.; Dmochowski, I. J. *J. Inorg. Biochem.* **2015**, *150*, 182−188. (b) Tang, X.; Zhang, J.; Sun, J.; Wang, Y.; Wu, J.; Zhang, L. *Org. Biomol. Chem.* **2013**, *11*, 7814−7824. (c) Bort, G.; Gallavardin, T.; Ogden, D.; Dalko, P. I. *Angew. Chem., Int. Ed.* **2013**, *52*, 4526−4537.

(13) (a) Luo, D.; Saltzman, W. M. *Nat. Biotechnol.* **2000**, *18*, 33−37. (b) Patil, S. D.; Rhodes, D. G.; Burgess, D. J. *AAPS J.* **2005**, *7*, E61−77. (c) Bishop, C. J.; Kozielski, K. L.; Green, J. J. *J. Controlled Release* **2015**, *219*, 488−499.

(14) Dobson, J. *Nat. Nanotechnol.* **2008**, *3*, 139−143.

(15) (a) Wang, N.; Butler, J. P.; Ingber, D. E. *Science* **1993**, *260*, 1124−1127. (b) Meyer, C. J.; Alenghat, F. J.; Rim, P.; Fong, J. H.-J.; Fabry, B.; Ingber, D. E. *Nat. Cell Biol.* **2000**, *2*, 666−668.

(16) (a) Bausch, A. R.; Hellerer, U.; Essler, M.; Aepfelbacher, M.; Sackmann, E. *Biophys. J.* **2001**, *80*, 2649−2657. (b) Bausch, A. R.; Möller, W.; Sackmann, E. *Biophys. J.* **1999**, *76*, 573−579. (c) Glogauer, M.; Ferrier, J. *Pfluegers Arch.* **1997**, *435*, 320−327.

(17) Hughes, S.; McBain, S.; Dobson, J.; El Haj, A. J. J. *J. R. Soc., Interface* **2008**, *5*, 855−863.

(18) (a) Kolpashchikov, D. M. *ChemBioChem* **2007**, *8*, 2039−2042. (b) Mokany, E.; Bone, S. M.; Young, P. E.; Doan, T. B.; Todd, A. V. *J. Am. Chem. Soc.* **2010**, *132*, 1051−1059. (c) Gerasimova, Y. V.; Cornett, E.; Kolpashchikov, D. M. *ChemBioChem* **2010**, *11*, 811−817. (d) Gerasimova, Y. V.; Kolpashchikov, D. M. *Angew. Chem., Int. Ed.* **2013**, *52*, 10586−10588.

(19) Bumb, A.; Brechbiel, M. W.; Choyke, P. L.; Fugger, L.; Eggeman, A.; Prabhakaran, D.; Hutchinson, J.; Dobson, P. J. *Nanotechnology* **2008**, *19*, No. 335601.

(20) (a) Gref, R.; Lück, M.; Quellec, P.; Marchand, M.; Dellacherie, E.; Harnisch, S.; Blunk, T.; Müller, R. H. *Colloids Surf., B* **2000**, *18*, 301−313.

(21) Cheng, G. Z.; Chan, J.; Wang, Q.; Zhang, W. Z.; Sun, C. D.; Wang, L. H. *Cancer Res.* **2007**, *67*, 1979−1987.

(22) Watanabe, O.; Imamura, H.; Shimizu, T.; Kinoshita, J.; Okabe, T.; Hirano, A.; Yoshimatsu, K.; Konno, S.; Aiba, M.; Ogawa, K. *Anticancer Res.* **2004**, *24*, 3851−3856.

(23) Li, Y.; Wang, W.; Wang, W.; Yang, R.; Wang, T.; Su, T.; Weng, D.; Tao, T.; Li, W.; Ma, D.; Wang, S. *Gynecol. Oncol.* **2012**, *124*, 112−118.

(24) Plank, C.; Schillinger, U.; Scherer, F.; Bergemann, C.; Rémy, J.-S.; Krötz, F.; Anton, M.; Lausier, J.; Rosenecker, J. *Biol. Chem.* **2003**, *384*, 737−747.

(25) Nguyen, J.; Szoka, F. *Acc. Chem. Res.* **2012**, *45*, 1153−1162.

DOI: 10.1021/jacs.7b06022
J. Am. Chem. Soc. 2017, 139, 12117−12120